Journal of Inorganic and General Chemistry
ZAAC
Zeitschrift für anorganische und allgemeine Chemie
DOI: 10.1002/zaac.202100035
ARTICLE

The Coordination Polymer $Cr(en)_2As_2VO_7$ Consisting of Alternating VO_4 Tetrahedra and As_2O_5 Handles Decorated by Cr^{3+} Centered Complexes

Maren Rasmussen,[a] Christian Näther,[a] and Wolfgang Bensch*[a]

Dedicated to Professor Christoph Janiak on the occasion of his 60th birthday

The new coordination polymer $Cr(en)_2As_2VO_7$ (en = ethylenediamine) was synthesized under solvothermal conditions as deep red crystals. In the crystal structure VO_4 tetrahedra and As_2O_5 handles formed by corner-sharing of two AsO_3 pyramidal units are joined by common oxygen atoms into an undulated chain that is directed along the crystallographic b-axis. The chain is decorated by $[Cr(en)_2]^{3+}$ complexes with the Cr^{3+} cation having bonds to two terminal O^{2-} anions of the As_2O_5 moiety thus generating a CrN_4O_2 octahedron, which displays a cis-configuration. The connection mode between Cr^{3+} and As_2O_5 leads to formation of a six-membered $CrAs_2O_3$ ring. The chains are arranged in a layer-like fashion in the (001) plane and these layers are stacked along [001]. A large number of N–H···O and C–H···O hydrogen bonds generate a three dimensional network. A Hirshfeld surface analysis was performed for visualizing the extended interchain interactions. The hydrogen bonding interactions are clearly detected in the IR spectrum. The UV-Vis spectrum shows an absorption at 2.3 eV which is in agreement with the red color of the sample.

Introduction

Since the discovery of the first high-nuclearity arsenato-polyoxovanadate (As-POV) $K_6[V_{15}As_6O_{42}(H_2O)]\cdot 8H_2O$[1] the chemistry of As-POVs was systematically developed.[2] New cluster types like in e.g. $[H_3KV_{12}As_3O_{39}(AsO_4)]^{6-}$,[3] $[V_{12}As_8O_{40}(HCO_2)]^{3-}$,[4] $[V_{16}As_4O_{42}]^{8-}$,[5] $[V_{14}As_8O_{42}(SO_3)]^{6-}$,[6] or $[As_8V_6O_{26}]^{4-}$[7] increased the structural and chemical variety of As-POVs. The chemistry could be further enhanced by e.g. decoration of the cluster anions by transition metal complexes[8–16] or by integration of transition metal cations into the cluster shell.[17,18] The latter cluster modification was also reported for a variety of POVs.[19] In compounds, which are chemically modified by transition metal cations or decorated by transition metal complexes, late transition metals were used in the syntheses or preformed complexes were applied. Many of the above mentioned transition metal complexes containing As-POVs were synthesized under solvothermal conditions mainly using V_2O_5 or NH_4VO_3 and As_2O_3 as starting materials. The high-nuclearity structures are than formed by self-assembly processes and in most cases the chemical composition of the products has no direct relation to the ratio of V:As:TM (TM = transition metal) applied in the reaction mixture. This observation can be traced back to the complexity of the solvothermal approach where frequently a large number of syntheses are necessary for finding the optimal conditions for high yields of the desired product. Until now, no As-POVs were reported containing either Cr^{3+} centered complexes for charge compensation or decorating the cluster shell. In our ongoing work we tried to prepare under solvothermal conditions a Cr^{3+} containing As-POV, but the products of several syntheses contained always the coordination polymer $Cr(en)_2As_2VO_7$. Here we report the synthesis, the crystal structure and selected properties of this new compound.

Results and Discussion

The new coordination polymer was solvothermally synthesized under basic conditions (pH = 11.6) in an attempt to prepare a high-nuclearity As-POV containing a Cr^{3+} centered complex. Under these conditions, normally the V^{5+} cation of the NH_4VO_3 educt is reduced to V^{4+} which is in a five-fold coordination of a square pyramidal environment. Mixed-valence As-POVs containing V^{5+}/V^{4+} were obtained at lower pH values and mainly under relatively mild conditions, see e.g.[20–22] Hence, it is surprising that the oxidation state of V was preserved and that $[VO_4]^{3-}$ tetrahedra were 'cut-out' from the $[VO_3]_\infty$ chains that are present in the crystal structure of NH_4VO_3.[23]

The title compound crystallizes in the monoclinic space group $P2_1/c$ with all atoms located in general positions. The

[a] M. Rasmussen, C. Näther, W. Bensch
Institute of Inorganic Chemistry,
Christian-Albrechts-University of Kiel,
Max-Eyth-Str. 2, 24118 Kiel, Germany
Tel.: +49 431 880–2419
Fax: +49 431 880–1520
E-mail: wbensch@ac.uni-kiel.de

Supporting information for this article is available on the WWW under https://doi.org/10.1002/zaac.202100035

© 2021 The Authors. Zeitschrift für anorganische und allgemeine Chemie published by Wiley-VCH GmbH. This is an open access article under the terms of the Creative Commons Attribution Non-Commercial License, which permits use, distribution and reproduction in any medium, provided the original work is properly cited and is not used for commercial purposes.

unique V atom is in a tetrahedral environment of four O^{2-} anions (Figure 1) and the two unique As^{3+} cations are each in a trigonal-pyramidal surrounding of three O^{2-} anions. Two AsO_3 groups are joined through a common corner to form an As_2O_5 unit. The VO_4 tetrahedra and the As_2O_5 moieties are connected by As–O–V bonds thus generating an undulated chain which is directed along [010]. The chain is decorated by Cr^{3+} centered complexes via Cr–O bonds to two O^{2-} anions of the As_2O_5 group (Figure 1). The connection mode generates a six-membered $CrAs_2O_3$ ring with Cr···As distances of 3.328 and 3.301 Å. The coordination environment of the Cr^{3+} cations is completed by two bidentate en ligands to form a CrN_4O_2 octahedron, with the O^{2-} anions in *cis*-position. The Cr–O bonds at 1.912(4) and 1.919(4) and the Cr–N bonds between 2.078(5) and 2.115(5) Å are in the typical range observed in literature[24,25] The CrN_4O_2 octahedron is slightly distorted as evidenced by the N–Cr–N, N–Cr–O and O–Cr–O angles (Table S1). We note that the Cambridge Structural Database does not contain crystal structures with $Cr(en)_2O_2$ moieties bonded to a semimetal or to a transition metal. The V–O bond lengths are between 1.635(4) and 1.823(4) Å, whereby two short bonds are formed to the terminal O^{2-} anions indicating some double-bond character as observed for the vanadyl group $(V{=}O)^{2+}$ and/or the bonds may be shortened by relatively strong electrostatic interactions. The two longer bonds are observed for the V–O–As bridges. The O–V–O angles range from 106.1 to 112.0° indicating a moderate distortion from ideal tetrahedral geometry. The geometric parameters are comparable to those reported for metavanadates like e.g. $[PPh_4]_2V_4O_{11}$ (PPh_4 = tetraphenylphosphonium),[26] in α,β-$(H_3N(CH_2)_2NH_3)[V_4O_{10}]$,[27] or in NH_4VO_3.[23] The bond valence sum (BVS) for the V center is 5.05 justifying the assignment of the oxidation state +5. The As–O bond lengths are divided into two long bonds for the As-O–V and As-O–As connections (1.792(4) – 1.838(4) Å) and two shorter bonds are found (1.697(4) and 1.698(4) Å) to O^{2-} anions, which are also bonded to Cr^{3+} cations. The sum of the covalent radii of As and O of 1.85 Å (r_{As} = 1.19 and r_O = 0.66 Å)[28] indicates that the two short bonds are stronger than a single bond which may be caused by strong electrostatic interactions. The bond valence sum for the two As^{3+} cations are 3.00 and 3.06 using the data for R_0 and b given in Ref.[29] supporting the assignment of the oxidation state +3. We note that the As–O bonding pattern observed in the title compound is different to that found in As-POVs, where the As–O bonds vary in a narrow range of ≈1.75 to 1.80 Å. Beside in As-POVs, the As_2O_5 moiety is also observed in complexes like in $[(LM)_2(As_2O_5)]$ (L = C_6H_3-2,6-$(CH_2NMe_2)_2$; M = Sb, Bi),[30] in arsenanes,[31] or is integrated in calixarenes.[32] But the As–O bonds in these compounds do not differ from that reported for As-POVs. For the As2 atom a relatively short intramolecular separation to one of the H atoms of a CH_2 group is observed with the As···H distance of 2.875 Å, slightly shorter than the sum of the van der Waals radii of 2.95 Å.[33]

The chains are arranged in a layer like fashion parallel to the (001) plane (Figure 2) and these layers are stacked along [001]. Hydrogen bonding interactions are observed between the N–H and C–H hydrogen atoms and the O atoms of neighbored chains in which all O atoms except the two having a bond to the Cr^{3+} cation are involved (Figure S1, Table S2). Two of the N–H hydrogen atoms are engaged in bifurcated hydrogen bonds. There are also two intrachain N–H···O bonds with H···O distances (Figure 1) of 2.328 and 2.269 Å and corresponding N–H···O angles 153.6 and 149.6 ° indicating strong interactions.

Weak intermolecular interactions can be analyzed in detail using the Hirshfeld surface approach[34–37] using the program Crystal Explorer 17.[38]

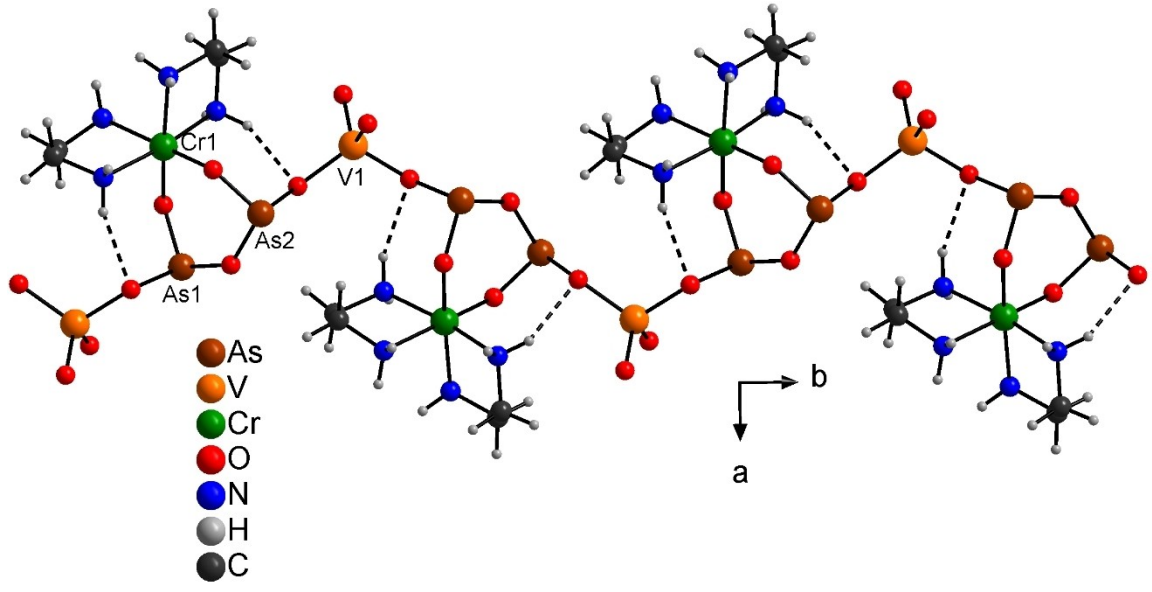

Figure 1. Part of the chain composed of alternating VO_4 tetrahedra and As_2O_5 groups decorated by the Cr^{3+} centered complexes. The broken lines indicate intrachain N–H···O bonds. Only selected atoms are labelled.

© 2021 The Authors. Zeitschrift für anorganische und allgemeine Chemie published by Wiley-VCH GmbH.

The Hirshfeld surface is mapped over d_{norm} which is calculated according to

$$d_{norm} = \frac{d_i - r_i^{vdW}}{r_i^{vdW}} + \frac{d_e - r_e^{vdW}}{r_e^{vdW}}$$

with d_i is the distance of a point on the surface to the nearest nucleus inside the surface, d_e is the distance from such a point to the next neighbor outside the surface, and vdW is the abbreviation for van der Waals radius. Red areas on the Hirshfeld surface (Figure 3, left) denote short distances and green to blue indicate long distances. For the present analysis an asymmetric unit of the chain was calculated by the program which leads to deep red areas in the bottom right of the Hirshfeld surface because two O atoms having covalent bonds to the V atom are not included in this asymmetric unit (Figure 3, left). In any case, there are several red areas on the surface which are caused by short interchain interactions. A detailed picture of these interactions is obtained using the fingerprint plot, which is a 2D representation of the Hirshfeld surface (Figure 3, right). The two spikes located at $d_i/d_e = 1.1$ Å/0.7 Å and $d_e/d_i = 0.7$ Å/1.1 Å are caused by O···H respectively H···O bonding representing 17.6% and 22.4% of the interchain interactions. The broad area between $d_i/d_e = 1.1$ Å/1.1 Å up to 1.4 Å/1.4 Å covers H···H interaction (31.3%). Beginning at $d_i/d_e =$ 1.78 Å/1.05 Å the weak As···H interactions are located. The two sharpest spikes are due to covalent V–O bonds as mentioned above.

In the IR spectrum of the en ligand one can expect different absorptions for the $-NH_2$ group: symmetrical stretching, asymmetrical stretching, bending, wagging, twisting, and rocking modes.[39] The IR spectrum of the title compound (Figure 4) shows three well resolved signals at 3251, 3149 and 3075 cm^{-1} and a shoulder at 3197 cm^{-1} in the region of the N–H

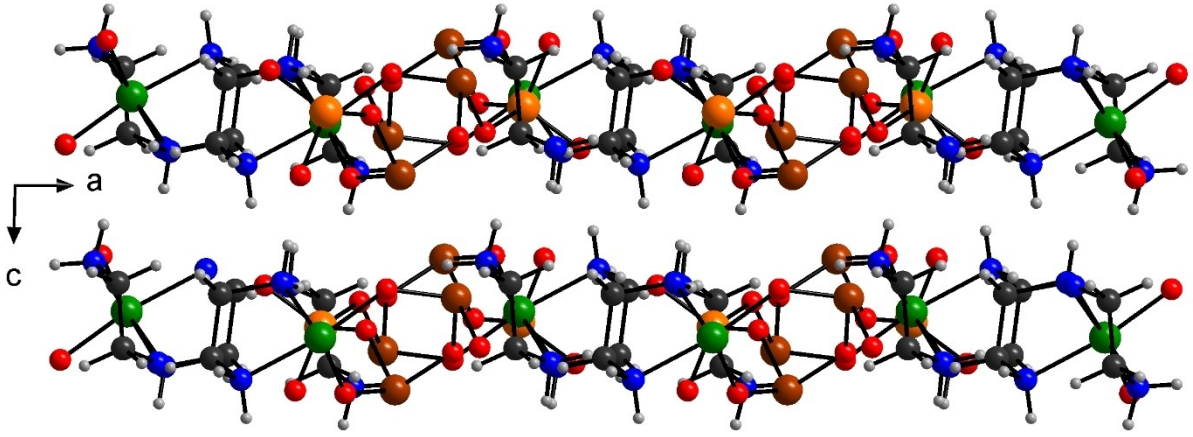

Figure 2. View of the layer like arrangement of the chains in the structure of the title compound.

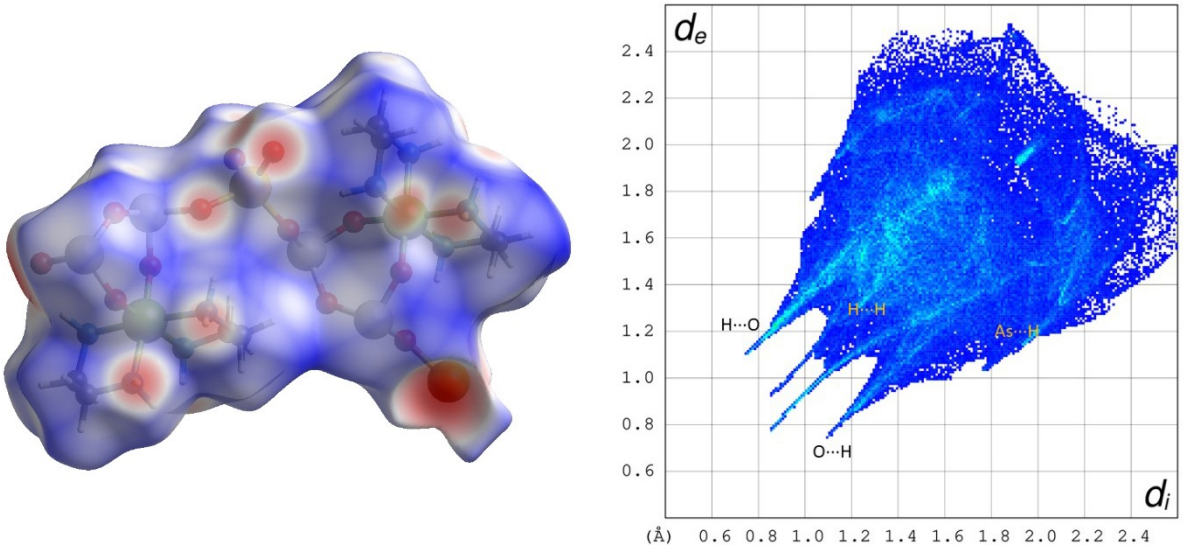

Figure 3. (left) The Hirshfeld surface of the asymmetric unit of the title compound; (right) The fingerprint plot derived from the Hirshfeld surface. The most prominent intermolecular interactions are indicated in the plot.

© 2021 The Authors. Zeitschrift für anorganische und allgemeine Chemie published by Wiley-VCH GmbH.

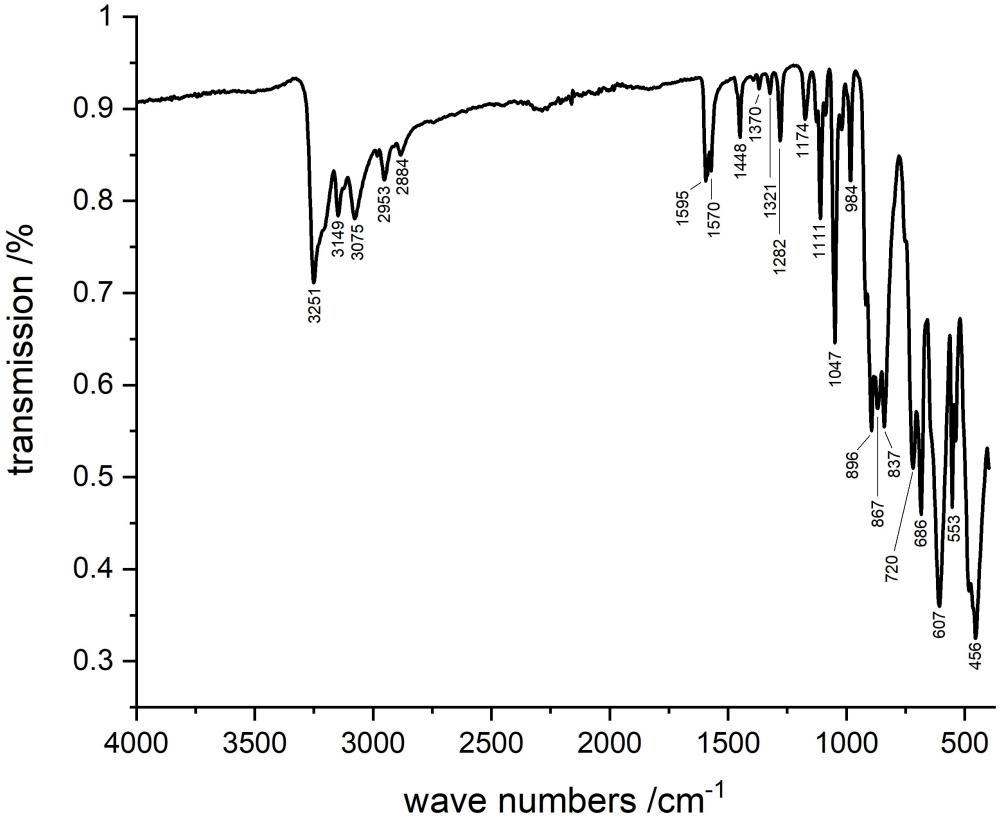

Figure 4. The IR spectrum of the title compound with wave numbers indicated for selected absorptions.

asymmetric and symmetric stretching modes. For solid en two absorptions were reported at 3332 and 3170 cm^{-1}.[40] The shift of the peaks to lower wave numbers and the occurrence of more than two signals is caused by bond formation to the Cr^{3+} cation and the presence of N–H···O interactions of different strengths and numbers. For a number of organic compounds it was demonstrated that the shift of the N–H absorptions depends on the N–H···O distance and can be larger than 200 cm^{-1}.[41]

The asymmetric and symmetric C–H modes are located at 2953 and 2884 cm^{-1}. The bending vibration of $–NH_2$ is found at 1595 and 1570 cm^{-1}, which is split and occur at lower wave numbers compared to solid en (1606 cm^{-1}),[40] which can be explained with the N–H···O hydrogen bonding discussed above. The CH_2 bending vibration is observed at 1150 cm^{-1}, a CH_2 deformation mode appears at 1148 cm^{-1} and the signal at 1282 cm^{-1} is most probable caused by a CH_2 twisting vibration. The twisting vibrations of the NH_2 groups are located at 1111 cm^{-1} and as a weak band at 1089 cm^{-1}. The relatively strong absorption at 1047 cm^{-1} may be assigned to a ring skeletal vibration[42] or C–N/C–C stretching modes.[39] For the $[VO_4]^{3-}$ anion with T_d symmetry four vibrations can be expected of which two are IR active. The reduction of the local symmetry as observed for the present anion removes the degeneracy of the bands and all four bands are IR active.[43] E.g., for $Mg_3(VO_4)_2$ four absorptions are observed in the region 950–800 cm^{-1}.[44] Because in this region also several vibrations of the en ligands are expected according to literature data[34,37] and As–O as well as V–O–As vibrations are found in this region an unambiguous assignment is not easy. But comparing the region of ≈850 and 500 cm^{-1} of IR spectra of As–POVs with that of the title compound some remarkable similarities can be observed. In this region ν_{as}(V–O–As) and ν_s(As–O) vibrations are located and values were reported as e.g. 835, 797, 685, and 606 cm^{-1} in.[45] In the title compound similar bands are observed at 837, 686 and 607 cm^{-1}, while the signal reported at 797 cm^{-1} can only be identified as a weak shoulder at 798 cm^{-1}. The remaining bands in the IR spectrum most probably are caused by more complex vibrations like chelate ring deformation, ν(Cr–N) plus ring deformation vibrations and CH_2/NH_2 rocking modes.

For the Cr^{3+} ($3d^3$) cation in an octahedral environment with the unpaired electrons in t^3_{2g} orbitals the $^4A_{2g}$ state is the ground state, and $^4T_{2g}$(F), $^4T_{1g}$(F) and $^4T_{1g}$(P) are the excited states. Hence, one can then expect three spin allowed transitions. If the symmetry is lower than O_h these bands split into two components. Generally, in the UV-Vis region the $^4A_{2g}(F) \rightarrow {}^4T_{2g}(F)$ transition is observed. The UV-Vis spectrum of the title compound (Figure 5) shows one absorption located at 2.3 eV (539 nm, 18551 cm^{-1}) caused by the $^4A_{2g}(F) \rightarrow {}^4T_{2g}(F)$ transition explaining the red color of the crystals. We note that for natural occurring ruby the electronic transition is located at about 2.27 eV (546 nm, 18300 cm^{-1}). A not well pronounced shoulder is observed at about 3.13 eV (396 nm, 25245 cm^{-1}) which may be explained by the $^4A_{2g}(F) \rightarrow {}^4T_{1g}(F)$ transition. The

© 2021 The Authors. Zeitschrift für anorganische und allgemeine Chemie published by Wiley-VCH GmbH.

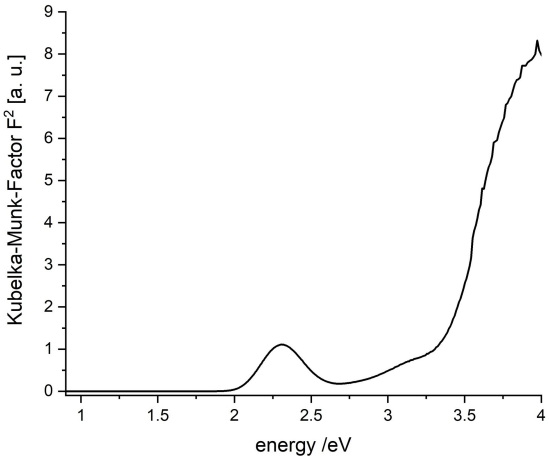

Figure 5. The UV-Vis spectrum of the title compound.

strong raise of the absorption at higher energies is most probably due to a charge-transfer transition.

The inverse magnetic susceptibility of the title compound yield a straight line over the measured temperature range (Figure S3). The data were fitted with the Curie-Weiss law yielding a value for the Curie constant of 1.87 cm^3 K/mol which matches very good with the expected spin-only value of 1.875 cm^3 K/mol for three unpaired spins. From the Curie constant the magnetic moment of 3.87 μ_B for the Cr^{3+} cation is calculated. The Weiss constant $\theta = -0.91(5)$ K clearly indicates negligible magnetic exchange interactions, i.e. the magnetic moments are isolated.

Conclusions

The solvothermal synthesis afforded crystallization of an unusual coordination polymer constructed by three different building units. The As_2O_5 moiety acts as tetradentate node joining VO_4 units and a Cr^{3+} centered complex generating an undulated chain. The formation of the compound is surprising because under the basic conditions applied here, the V^{5+} cation is normally reduced to V^{4+} as observed for a large number of arsenato polyoxovanadates. The detailed investigation of the interchain interactions performed with a Hirshfeld surface analysis demonstrates the importance of hydrogen bonding involving strong N–H···O bonds. These interactions affect mainly the NH_2 related vibrations in the IR spectrum. The UV-Vis spectrum shows one electronic transition, which explains the red color of the title compound. The evaluation of the magnetic data show that the Cr^{3+} cation is magnetically isolated.

Experimental Details

Synthesis

In a glass tube with a volume of 11 mL, 1.34 mmol (156.8 mg) NH_4VO_3, 1.194 mmol As_2O_3 (236.3 mg) and 0.66 mmol (175.89 mg) $CrCl_3 \cdot 6H_2O$ were reacted in a solution of 1.7 mL ehtylenediamine and 2.3 mL H_2O (pH = 11.6) for 5d at 150 °C. The reaction product contained red needles which were filtered off and washed with water and acetone. The yield was about 35 % based on NH_4VO_3.

Single crystal structure analysis: Data collection was performed using an Imaging Plate Diffraction System (IPDS-2) from Stoe&Cie with Mo-Kα radiation. A numerical absorption correction was performed using X-Red and X-Shape of the software package X-Area.[46] STOE&CIE GmbH, Darmstadt (Germany).The structures were solved with SHELXT[47] and structure refinement was performed against F^2 using SHELXL-2018.[48] The C–H and N–H hydrogen atoms were positioned with idealized geometry and were refined isotropic with U_{iso} (H) = 1.2 U_{eq} (C) using a riding model. The crystal is non-merohedrally twinned, which leads to very poor reliability factors (R1 for all reflections with $F_o > 4\sigma(F_o) = 0.0944$ and wR2 for all data = 0.3405). Therefore a twin refinement using data in HKLF-5 format was performed leading to a BASF parameter of 0.213(3) and resulting in much better reliability factors (Table S3). Selected crystal data and details of the structure refinements are given in Table S3 and a numbering scheme of the atoms is shown in Figure S2.

CCDC 2057176 contain the supplementary crystallographic data for this paper. These data can be obtained free charge from the Cambridge Crystallographic Data Centre via http://www.ccdc.cam.ac.uk/data_request/cif.

Characterization

Powder X-ray Diffraction (PXRD): The powder diffraction pattern was collected on a STOE Stadi-P diffractometer (Cu-$K_{\alpha 1}$ radiation, $\lambda = 1.540598$ Å) equipped with a MYTHEN 1 K detector (DECTRIS). The experimental and the calculated patterns match perfectly indicating the phase purity of the samples (Figure S4).

Energy Dispersive X-ray Spectroscopy (EDX): EDX analysis was carried out on a Philips Environmental Scanning Electron Microscope ESEM XL30 equipped with an EDX detector. Average atomic ratio measured on six crystals: Cr:As:V = 0.98:1.97:1.03

Infrared Spectroscopy: The infrared spectrum was recorded at room temperature from 80 to 6000 cm^{-1} with a Bruker Vertex70 FT-IR spectrometer.

UV/Visible Spectroscopy: UV/Vis measurement was done at room temperature using an UV/Vis/NIR two channel spectrometer Cary 5 (Varian Techtron Pty., Darmstadt, 200–3000 cm^{-1}). Powdered $BaSO_4$ was used as white standard. The UV/Vis data were converted using the Kubelka-Munk function.

Measurement of magnetic data was performed with a Quantum Design PPMS-9 device. The sample (36.0 mg) was placed in a gelatin capsule and data were recorded in the field cooled mode between 300 and 4.2 K with an external field H = 1 T. The raw data were corrected for core diamagnetism using Pascal's increments.

© 2021 The Authors. Zeitschrift für anorganische und allgemeine Chemie published by Wiley-VCH GmbH.

Acknowledgments

Financial support by the State of Schleswig-Holstein is gratefully acknowledged. Open access funding enabled and organized by Projekt DEAL.

Keywords: coordination polymer · solvothermal synthesis · crystal structure · spectroscopy · Hirshfeld surface analysis

[1] A. Müller, J. Döring, *Angew. Chem. Int. Ed. Engl.* **1988**, *27*, 1721.
[2] K. Yu. Monakhov, W. Bensch, P. Kögerler, *Chem. Soc. Rev.* **2015**, *44*, 8443—8483.
[3] A. Müller, M. Penk, J. Döring, *Inorg. Chem.* **1991**, *30*, 4935–4939.
[4] D. Gatteschi, B. Tsukerblatt, A.-L. Barra, L. C. Brunei, A. Müller, J. Döring, *Inorg. Chem.* **1993**, *32*, 2114–2117.
[5] S.-T. Zheng, J. Zhang, B. Li, G.-Y. Yang, *Dalton Trans.* **2008**, 5584–5587.
[6] A.-L. Barra, D. Gatteschi, L. Pardi, A. Müller, J. Döring, *J. Am. Chem. Soc.* **1992**, *114*, 8509–8514.
[7] E. Dumas, C. Livage, S. Halut, G. Herve, *Chem. Commun.* **1996**, 2437–2438.
[8] W.-M. Bu, G.-Y. Yang, L. Ye, J.-Q. Xu, Y.-G. Fan, *Chem. Lett.* **2000**, *29*, 462–463.
[9] S.-T. Zheng, J. Zhang, G.-Y. Yang, *Eur. J. Inorg. Chem.* **2004**, 2004–2007.
[10] S.-T. Zheng, Y.-M. Chen, J. Zhang, G.-Y. Yang, *Z. Anorg. Allg. Chem.* **2006**, *632*, 155–159.
[11] S.-T. Zheng, Y.-M. Chen, J. Zhang, J.-Q. Xu, G.-Y. Yang, *Eur. J. Inorg. Chem.* **2006**, 397–406.
[12] B.-X. Dong, J. Peng, C. J. Gomez-Garcia, S. Benmansour, H.-Q. Jia, N.-Hai Hu, *Inorg. Chem.* **2007**, *46*, 5933–5941.
[13] H.-Y. Guo, Z.-F. Li, X. Zhang, L.-W. Fu, Y.-Y. Hu, L.-L. Guo, X.-B. Cui, Q.-S. Huo, J.-Q. Xu, *CrystEngComm* **2016**, *18*, 566–579.
[14] H.-Y. Guo, T.-T. Zhang, P.-H. Lin, X. Zhang, X.-B. Cui, Q.-S. Huo, J.-Q. Xu, *CrystEngComm* **2017**, *19*, 265–275.
[15] A. Wutkowski, C. Näther, J. van Leusen, P. Kögerler, W. Bensch, *Z. Naturforsch.* **2014**, *69b*, 1306–1314.
[16] L. K. Mahnke, G. Stehlíková, K. Synnatschke, C. Backes, C. Näther, W. Bensch, *ChemNanoMat* **2021**, *7*, 78–84.
[17] S.-T. Zheng, J. Zhang, J.-Q. Xu, G.-Y. Yang, *J. Solid State Chem.* **2005**, *178*, 3740–3746.
[18] Y. Qi, Y. Li, E. Wang, Z. Zhang, S. Chan, *Dalton Trans.* **2008**, 2335–2345.
[19] M. Anjass, G. A. Lowe, C. Streb, *Angew. Chem. Int. Ed.* **2020**, doi.org/10.1002/anie.202010577-.
[20] R. Basler, G. Chaboussant, A. Sieber, H. Andres, M. Murrie, P. Kögerler, H. Bögge, D. C. Crans, E. Krickemeyer, S. Janssen, H. Mutka, A. Müller, H.-U. Güdel, *Inorg. Chem.* **2002**, *41*, 5675–5685.
[21] A. Müller, J. Döring, *Z. Anorg. Allg. Chem.* **1991**, *595*, 251–274.
[22] A. Müller, J. Döring, M. I. Khan, V. Wittneben, *Angew. Chem. Int. Ed. Engl.* **1991**, *30*, 210–212.
[23] A. Perez-Benitez, S. Bernes, *IUCrData* **2018**, *3*, x181080.
[24] K. Kaas, *Acta Crystallogr.* **1979**, *B35*, 596–599.
[25] F. Rominger, U. Thewalt, *Z. Naturforsch.* **1996**, *51b*, 1716–1724.
[26] S. Sharma, A. Ramanan, P. Y. Zavalij, M. S. Whittingham, *CrystEngComm* **2002**, *4*, 601–604.
[27] Y. Zhang, R. C. Haushalter, A. Clearfield, *Inorg. Chem.* **1996**, *35*, 4950–4956.
[28] B. Cordero, V. Gomez, A. E. Platero-Prats, M. Reves, J. Echeverria, E. Cremades, F. Barragan, S. Alvarez, *Dalton Trans.* **2008**, 2832–2838.
[29] O. C. Gagne, F. C. Hawthorne, *Acta Crystallogr.* **2015**, *B71*, 561–578.
[30] T. Svoboda, R. Jambor, A. Ruzicka, R. Jirasko, A. Lycka, F. De Proft, L. Dostal, *Organometallics* **2012**, *31*, 1725–1729.
[31] M. A. Said, K. C. K. Swamy, M. Veith, V. Huch, *J. Chem. Soc.-Perkin Trans.* **1995**, *1*, 2945–2951.
[32] S. Shang, D. V. Khasnis, H. Zhang, A. C. Small, M. Fan, M. Lattman, *Inorg. Chem.* **1995**, *34*, 3610–3615.
[33] M. Mantina, A. C. Chamberlin, R. Valero, C. J. Cramer, D. G. Truhlar, *J. Phys. Chem. A* **2009**, *113*, 5806–5812.
[34] M. A. Spackman, D. Jayatilaka, *CrystEngComm* **2009**, *11*, 19–32.
[35] M. A. Spackman, J. J. McKinnon, D. Jayatilaka, *CrystEngComm* **2008**, *10*, 377–388.
[36] A. J. Edwards, C. F. Mackenzie, P. R. Spackman, D. Jayatilaka, M. A. Spackman, *Faraday Discuss.* **2017**, *203*, 93–112.
[37] M. A. Spackman, J. J. McKinnon, *CrystEngComm* **2002**, *4*, 378–392.
[38] M. J. Turner, J. J. Mckinnon, S. K. Wolff, D. J. Grimwood, P. R. Spackman, D. Jayatilaka, M. A. Spackman, *Crystal Explorer 17* **2017**. The University of Western Australia.
[39] M. E. Baldwin, *J. Chem. Soc.* **1960**, 4369–4376.
[40] M. G. Giorgini, M. R. Pelletti, G. Paliani, R. S. Cataliotti, *J. Raman Spectrosc.* **1983**, *14*, 16–21.
[41] K. Nakamoto, M. Margoshes, R. E. Rundle, *J. Am. Chem. Soc.* **1955**, *77*, 6480–6486.
[42] D. B. Powell, N. Sheppard, *Spectrochim. Acta* **1961**, *17*, 68–76.
[43] R. L. Frost, S. J. Palmer, J. Cejka, J. Sejkora, J. Plasil, S. Bahfenne, E. C. Keeffe, *J. Raman Spectrosc.* **2011**, *42*, 1701–1710.
[44] G. Busca, *J. Raman Spectrosc.* **2002**, *33*, 348–358.
[45] A. Müller, J. Döring, H. Bögge, *J. Chem. Soc. Chem. Commun.* **1991**, 273–274
[46] Stoe&Cie **2008**, X-AREA, Version 1.44.
[47] G. M. Sheldrick, *Acta Crystallogr.* **2015**, *A71*, 3–8.
[48] G. M. Sheldrick, *Acta Crystallogr.* **2015**, *C71*, 3–8.

Manuscript received: January 29, 2021
Revised manuscript received: March 6, 2021
Accepted manuscript online: March 16, 2021

 © 2021 The Authors. Zeitschrift für anorganische und allgemeine Chemie published by Wiley-VCH GmbH.